A multivariate statistical method for susceptibility analysis of the debris flow in Southwest China

Feng Ji[1], Zili Dai[2], Renjie Li[1]

[1]State Key Laboratory of Geohazard Prevention and Geoenvironment Protection, Chengdu University of Technology, Chengdu, 610059, China

[2]Department of Civil Engineering, Shanghai University, 99 Shangda Road, Shanghai, 200444, China

Correspondence to: Zili Dai (87zili.dai@gmail.com)

Abstract. Southwest China is characterized by many steep mountains and deep valleys due to the uplift activity of the Tibetan Plateau. The 2008 Wenchuan Earthquake left large amounts of loose materials in this area, making it a severe disaster zone in terms of debris flow. Susceptibility is a significant factor of debris flow for evaluating its formation and impact. Therefore, it is in urgent need to analyze the susceptibility of debris flows in this area. To quantitatively predict the susceptibility of debris flows, this study evaluates 70 typical debris flow gullies as statistical samples, which are distributed along the Brahmaputra River, Nujiang River, Yalong River, Dadu River, and Ming River respectively. Nine indexes are chosen to construct a factor index system and then to evaluate the susceptibility of debris flow. They are the catchment area, longitudinal gradient, average gradient of the slope on both sides of the gully, catchment morphology, valley orientation, loose material reserves, location of the main loose material, antecedent precipitation, and rainfall intensity. Then, an empirical model based on the quantification theory type I is established for the susceptibility prediction of debris flows in Southwest China. Finally, 10 debris flow gullies on the upstream of the Dadu River are analyzed to verify the reliability of the proposed model. The results show that the accuracy of the statistical model is 90%.

1 Introduction

Debris flows are a common geological hazard in mountainous areas, which transport large amounts of sediment down-slope and cause serious damage to dwellings, roads, and other lifelines. China has mainly mountainous topography and is one of the most debris-flow prone countries in the world. Until March 2019, there are approximately 50,000 debris flows have occurred in China (Di et al. 2019). A significant percentage of these debris flows are distributed in Southwest China, particularly in the Wenchuan earthquake area, where large amounts of

loose material were produced by the earthquake-induced landslides (Xu et al. 2012; Huang et al. 2015; Dai et al. 2017).

Due to the complex nature of debris flows, it is quite difficult to fully understand their initiation mechanism and precisely forecast their occurrence (Brayshaw and Hassan, 2014). The uncertainty of debris flows poses significant threats to human lives in downstream areas (Schürch et al. 2011). Debris flow susceptibility expresses the occurrence possibility of debris flow in an area with respect to its geomorphologic characteristics (Kappes et al. 2011; Bertrand et al. 2013). Therefore, susceptibility analysis is an essential step to conduct the risk assessment of debris flow hazards (Di et al. 2019; Zou et al. 2019).

Debris flow susceptibility analyses include two steps: 1) identification of the potential source areas and 2) prediction of the possible deposition areas (Kang and Lee, 2018). In the literature, a large number of prediction models have been proposed for the susceptibility analyses of debris flows. For the first step, statistical models that use various environmental factors contributing to possible instabilities are well-established. For example, Blahut et al. (2010) performed susceptibility assessment for the source areas of landslide induced debris flows in the Valtellina Valley based on bivariate statistics. Bertrand et al. (2013) performed two multivariate statistical models, a linear discriminant analysis (LDA) and a logistic regression (LR), to analyze the debris flow susceptibility of upland catchments. Jomelli et al. (2015) proposed a Bayesian hierarchical probabilistic model to investigate how debris flows respond to environmental and climatic variables in the French Alps. Carrara et al. (2008) discussed the application of different statistical models to debris flows in Val di Fassa, Trento Province. Lucà et al. (2011) compare bivariate and multivariate statistical models for the evaluation of gullying susceptibility in Northern Calabria, South Italy, and concluded that multivariate statistical models were found to be the best model in predicting debris flow susceptibility of the study area. For the second step, the concept “angle of reach” was widely used in the empirical models to predict the runout distance of the debris flows (Hürlimann et al. 2012; Horton et al. 2013). Recently, many numerical models were proposed to simulate the propagation of the debris flows and predict the deposition area. For example, Pirulli and Sorbino (2008) analyzed the propagation of potential debris flows in Southern Italy using two numerical codes RASH3D and FLO2D. Beguería et al. (2009) proposed a two-dimensional model based on numerical integration of the depth-averaged motion equations to predict the debris flow propagation over complex terrain near Lienz, Eastern Tyrol, Austria. Huang et al. (2015) presented a numerical model based on

the smoothed particle hydrodynamic (SPH) method to calculate the runout distance of catastrophic debris flows that occurred in the Wenchuan Earthquake area. Gregoretti et al. (2016) used a cell model to simulate a debris flow that occurred on the Rio Lazer. Moraci et al. (2017) performed debris flow susceptibility zoning of debris flows in the Province of Reggio Calabria based on the SPH method. Some recent analysis methods of debris-flow susceptibility could be found in Cama et al. (2017), Prieto et al. (2018), and Rosatti et al. (2018).

The previous studies mentioned above have attempted to conduct debris flow susceptibility analysis in specified regions. Southwest China is characterized by steep mountains and deep valleys, and is strongly affected by the uplift activity of the Tibetan Plateau. Moreover, Southwest China has abundant loose material after the 2008 Wenchuan Earthquake. Therefore, a series of large-scale debris flows have been occurred during the rainy seasons in Southwest China (Wu et al. 2019). In the literature, many models for the debris flow risk prediction in this area have been proposed. For example, Xu et al. (2012) assess the debris flow susceptibility based on information value model and Geographic Information System (GIS) in Sichuan, China. Wang et al. (2016) adopted a self-organizing map method to analyze the susceptibilities of debris flows at the Wudongde Damsite in southwest China. Li et al. (2017) carried out a susceptibility analysis on debris flows also in the Wudongde dam area using the fuzzy C-means algorithm (FCM). Recently, Liu et al. (2018) presented a comprehensive risk assessment model based on semi-quantitative methods to quantify the risk level of each zone in Southwest China. Di et al. (2019) developed a gradient boosting machine (GBM) to predict the susceptibilities of debris flows in Southwest China. Wu et al. (2020) implemented logistical regression models to identify the areas that are susceptible to debris flow formations in Sichuan Province, China. Through the above researches, some promising results have been achieved concerning the susceptibility analysis of the debris flows in Southwest China. This work aims at providing a multivariate statistical method for susceptibility analysis of the debris flow in Southwest China. 70 debris flow gullies in Southwest China were analyzed, and nine key indicators were extracted through the initial analysis of the debris flows. Through multivariate statistics, an empirical formula of susceptibility was established, which was then validated with the data of the 10 debris flow gullies on the upstream of the Dadu River. It is worth noting that this work confines to identify the potential debris-flow source areas in Southwest China, neglecting the runout of the phenomena.

2 Characteristics of the debris flows in the study area

Southwest China is charactered by steep mountains and deep valleys and is strongly affected by the uplift activity of the Qinghai–Tibet Plateau. Furthermore, there is abundant loose material and rainfall in this area. Therefore, it is a severe disaster zone in terms of debris flow. In the past three years, 70 typical debris flows distributed along the Brahmaputra River, Nujiang River, Yalong River, Dadu River, and Ming River are investigated. The location of the debris flows is shown in Figure 1, and some typical debris flows are shown in Figure 2. Based on the field investigation, the characteristics of the five water catchments are summarized as follows.

1) In the upstream of the Brahmaputra River, 18 debris flow gullies along the Dagu River and Jiexu River reaches are investigated. The lithology in this area is the irruptive rock of the late Yanshanian–Himalayan epoch, with a wide distribution of granodiorite. The average annual rainfall in this area is about 540 mm and concentrates mostly in summer. Large-scale ice-melting-type debris flow once occurred in this region. However, in recent years, the debris flows in this area are mainly caused by precipitation. Material reserves are abundant in the valleys, whereas unstable materials are found less frequently and the deposit zone is small. It is found that most of the debris flows in this area are in the decline phase, and most debris flow gullies are in the low-frequency category.

2) In the midstream of the Nujiang River catchment, 11 debris flow gullies located in the Zuogong River section are investigated. The stratum mainly includes the Permian Nacuo group slate and Triassic Wapu group marble. As this region is located in the subtropical zone south of the Himalayas, it is characterized by a humid climate and plentiful precipitation. This leads to an extensive distribution of debris flow gullies.

3) In the midstream of the Yalong River catchment, 27 debris flow valleys are investigated, which belong to a plateau climate zone with complex meteorological and hydrological conditions. The concentricity and suddenness of rainfall provide hydraulic conditions for the debris flow breakouts. Collapses and landslides in the valley occur frequently, which provide abundant material resources for the debris flow occurrence. Moreover, the debris flow activity is intensified by unreasonable human engineering activities such as deforestation and accumulation of highway waste residues.

4) In the Dadu River catchment, 42 gullies in the midstream and the upstream are surveyed. This area is characterized by intense new tectonic movement, high earthquake intensity, and rock fragmentation on the mountain

surface. Debris flow, collapse, and other geological disasters are widely distributed, and the deposit zone of the debris flow is large. The maturity of the valley is high.

5) In the Minjiang River catchment, the Wenchuan River section are surveyed, and 32 debris flows are investigated. This region is characterized by abundant loose materials, frequent debris flows, and high possibility of the breakout of large-scale debris flows. Most of these debris flows are intensive in activity and have not declined in recent times.

3 Methodology

3.1 Investigation and statistical data

In total 70 debris flow gullies distributed in five water catchments in Southwest China were investigated from the gully outlet to the watershed over the past three years. This work includes the investigation of the watershed terrain, geological structure, outbreak scale, loose material distribution, processes of occurrence and movement, frequency of debris flows, and so on. The role of each factor causing instability of the source materials are analysed.

The antecedent precipitation can reduce the soil shear strength, and has an important influence on the formation and the scale of debris flows (Shieh et al. 2009). Therefore, the precipitation data before the outbreak of debris flows was collected from local meteorological bureaus, and used as one of the main influence factors to assess the susceptibility of debris flows in this study. In this work, the antecedent precipitation is classified into three categories: inadequacy, medium and adequacy. The classification criteria are listed in Table 1.

3.2 Field test

Bulk density tests and soil screening tests are carried out in the 70 debris flow deposit areas. Figure 3 shows the results of the bulk density tests. The bulk densities of the soil material in the debris flow deposits are mainly between 1.3 g/cm^3-1.8 g/cm^3, and the average bulk density is about 1.48 g/cm^3. The results of the screening test show that the material composition in the deposit zone is mainly composed of block gravel mixed soil, the content of the block gravel is 30-50%, the content of silt and clay is about 20-40%, and the rest of the deposit material is breccia. The reason for the high content of coarse stone soil is that the collapse phenomenon is quite common due to the active crustal movement in the study area.

3.3 Drilling and geophysical prospecting

The geologic condition in the active debris flow gullies in Southwest China is very complicated. To investigate the material composition and the thickness of the deposit area, the geological drilling was conducted in the active debris flow gullies along the Dadu River, Yalong River, Yaluzangbo River, and Minjiang River. The drilling information, such as the drilling location, drilling depth, and the soil characteristics are provided in Table 2.

3.4 Statistical technique

The statistical techniques can be grouped into bivariate and multivariate methods. A bivariate statistical method analyses each parameter individually, therefore the calculation and application in bivariate statistical models are straightforward and efficient (Suzen and Doyuran, 2004). On the other hand, a multivariate statistical method considers the interaction of all parameters in controlling the occurrence of a phenomenon, and is considered as one of the best methods in predicting debris flow susceptibility (Lucà et al. 2011). Hayashi's quantification theory is a well-known multivariate statistical method developed by Hayashi (1961). The quantification theory type I applies multiple linear regression methods, which can simultaneously process qualitative and quantitative variables, and evaluate the weight of each variable. Therefore, it is widely used in various fields (Matsumura 2004; Ishihara et al. 2008; Inoue et al. 2009; Shen and Chen, 2018). In this method, the qualitative and quantitative variables could be mutually transformed based on a reasonable principle. Therefore, this method has very good applicability to process the quantitative and qualitative influencing factors of debris flow risk.

In the Hayashi's quantification theory type I, qualitative variables are termed items. All possibilities for each item are termed categories. A dummy variable δ_i (j, k) is introduced in the method to express the response of an item and the category for each sample:

$$\delta_i(j,k) = \begin{cases} 1, & \text{if response of } i\text{th sample in the category } k \text{ of} \\ & \text{item } j \text{ to the corresponding external criterion;} \\ 0, & \text{otherwise.} \end{cases} \quad \begin{cases} i = 1, 2, \ldots, n; \\ j = 1, 2, \ldots, m. \end{cases} \tag{1}$$

where n is the number of samples and m denotes the number of items.

The response matrix X can be expressed as a $n \times p$-order matrix composed of all categories δ_i (j, k):

$$X=\begin{pmatrix} \delta_1(1,1)\cdots\delta_1(1,r_1) & \delta_1(2,1)\cdots\delta_1(2,r_2)\cdots\delta_1(m,1)\cdots\delta_1(m,r_m) \\ \delta_2(1,1)\cdots\delta_2(1,r_1) & \delta_2(2,1)\cdots\delta_2(2,r_2)\cdots\delta_2(m,1)\cdots\delta_2(m,r_m) \\ \vdots \quad\quad \vdots & \vdots \quad\quad\quad \vdots \quad\quad\quad \vdots \quad\quad\quad \vdots \\ \delta_n(1,1)\cdots\delta_n(1,r_1) & \delta_n(2,1)\cdots\delta_n(2,r_2)\cdots\delta_n(m,1)\cdots\delta_n(m,r_m) \end{pmatrix} \quad (2)$$

To establish a quantitative analysis model, the qualitative and quantitative in-situ observations are used to fit the linear relationship between the concerned independent variable and the dependent variable. In the Hayashi's quantification theory type I, the random variable changes with the *m* variables:

$$y_i=\sum_{j=1}^{m}\sum_{k=1}^{r_j}\delta_i\left(j,k\right)b_{jk}+\varepsilon_i,\quad i=1,2,...,n \quad (3)$$

where y_i represents the susceptibility of the *i*th debris flow gully. r_j is the number of categories of the item *j*. b_{jk} is a constant coefficient depending on category *k* in item *j*. ε_i is a random error.

To establish an analysis model of debris flow susceptibility, some necessary steps should be followed based on Hayashi's quantification theory type I: 1) building an index system; 2) selecting samples and assigning values; 3) establishing the analysis model using single slopes; 4) conducting a significance test of the regression equation and each variable, 5) applying this analysis model to regional debris flow hazards evaluation.

4 Model generation and results

4.1 Indexes and categories in the statistical model

There are many factors that affect the debris flow formation and development. From the perspective of source material of the debris flows, the main influence factors are catchment area, loose material position and loose material reserves. The antecedent precipitation and H1p rainfall intensity are the main generate conditions of debris flows. Besides, the catchment morphology, longitudinal gradient, average gradient of slope on both sides of the gully, and valley orientation are the main factors to affect the development of debris flows. Therefore, the above nine indexes (listed in Table 3) are selected in this study to assess the susceptibility of debris flows. Each factor is classified into certain categories according to the values shown in Table 4.

4.2 Sample quantification

70 debris flow gullies in Southwest China are selected as the sample to evaluate the performance of the statistical model. The detail information of these debris flow gullies is listed in Table 5. The values of the samples are assigned according to Eq. 1, and the response from each category is obtained. The sample data then can be transformed into a "0-1" reflection matrix.

4.3 Statistical model based on Hayashi's quantification theory

When the quantitative theory and regression analysis take the binary-state variables 0 and 1, the equation can be revised as the following linear regression expression:

$$y_i = a_0 + \sum_{j=1}^{f} a_j x_{ij} + \varepsilon_i \quad (i = 1, ..., n) \tag{4}$$

Based on Eq. 4 and matrix derivation regression calculation, the contribution values of each item are obtained, as shown in Table 6.

Substituting the numerical values in Eq. 4, the susceptibility prediction model of debris flow is established, which can be represented as follows:

$$\begin{aligned} Y = {} & 0.573x_{11} + 0.821x_{12} + 0.910x_{13} + 0.875x_{21} + 0.955x_{22} + 0.320x_{23} \\ & - 0.107x_{32} - 0.163x_{41} + 0.135x_{42} + 0.213x_{43} - 0.136x_{51} - 0.174x_{52} \\ & + 0.246x_{62} + 0.454x_{63} - 0.220x_{71} - 0.161x_{72} + 0.034x_{82} + 0.071x_{83} \\ & - 0.038x_{91} + 0.043x_{92} \end{aligned} \tag{5}$$

In Eq. 5, Y is the susceptibility for the debris flow, and the meanings of x_{11}, x_{12}, x_{13} and other indexes are detailed in Table 4. Based on the statistical analysis on the debris flows occurred in Southwest China, the susceptibility values are classified into three categories in the proposed model:

$$\begin{cases} Y < 1.5 & \text{Low susceptibility} \\ 1.5 \le Y < 2.5 & \text{Medium susceptibility} \\ Y \ge 2.5 & \text{High susceptibility} \end{cases} \tag{6}$$

5 Validation and discussion

5.1 Fitting degree analysis

R_2 is the fitting degree, which is widely used to evaluate the accuracy of prediction models. As shown in the Table 7, the fitting degree of the proposed model is 71.8%, which shows that this model can precisely predict the susceptibility of debris flows in Southwest China.

5.2 Self-test coincidence rate

The values of each index are used in the established model to calculate the predicted values of the susceptibility based on the Eq. 5, and then the predicted values are compared with the actual susceptibility. In this study, self-test coincidence rate is defined as the ratio of the predicted result to the actual susceptibility. As shown in Fig. 4, the predicted values of debris-flow susceptibility are graded. For the calculated results listed in Table 8, the prediction accuracy for the low susceptibility, medium susceptibility, and high susceptibility debris flows are 78.5%, 92.3%, 82.0%, respectively, which indicates that the proposed model can predict the debris-flow susceptibility well.

5.3 Residual error analysis

Residual error is the difference between a group of values observed and their arithmetical mean. As shown in Figure 5, the residual error of the model mainly fluctuates between ± 0.45, which indicates that the regression line can fit the field value well, and the residual frequency is approximately close to the normal distribution.

5.4 Verification of proposed model

The Kaka basin is located on the upper part of the Dadu River, southeast of the Qinghai–Tibet Plateau. The valley is deep and the river runs from north to south. The regional topography is characterized by high altitudes in the east and low altitudes in the west. The terrain is composed of high mountains with elevations of 2000 m. There are three layers of wide valley mesas, and the uplift of mountains and river erosion is significant in this area. The river elevation in the Kaka basin is approximately 1800 m, the river width is 140–185 m, and the slope angle is approximately 45–60°. The main faults are denoted as F1, F5, F5-1, F6, and F7 in Figure 6. The strike is NW, and they have a 40–60° angle with the river. A series of debris flow gullies have occurred in the basin.

10 typical debris flow gullies on the upstream of the Dadu River are selected as samples for the model validation (as shown in Figure 7, and listed in Table 9). The accuracy of the established model is verified through the comparison with field investigation results. Table 9 provides the relevant basic data for the samples. Each secondary index is transformed into a 0-1 mode, and all the samples are adopted to construct a 9 × 26 matrix. Table 10 shows the predicted susceptibility by the proposed model and the actual susceptibility obtained by the field investigation. The comparison shows that the accuracy rate of the model is 90%, and only the prediction result of the Linong gully deviates from the actual susceptibility. Therefore, detail field investigation was then carried out to analyze the debris flow susceptibility in the Linong gully.

Figure 8 shows the catchment of the Linong Gully. The total area of the catchment is about 10.09 km^2, and the total amount of loose material is about 4.04×10^6 m^3. The soil material, as shown in Figure 9, is mainly composed of block and crushed stone. Their particle sizes are generally 10-40 cm. In the calculation process, the catchment area is quite large, and then the loose material per catchment area is relatively very small, as shown in Figure 8. Based on the data, the prediction susceptibility of the Linong gully is 2.421, which is very close to the high susceptibility threshold value 2.5. Therefore, although there is a minor deviation, it can still be concluded that the proposed model can perform well to predict the debris flow susceptibility in Southwest China.

6 Conclusions

Debris flows frequently occurred in Southwest China and resulted in severe damage to dwellings and lifelines. Based on the Hayashi's quantification theory type I, an initiation susceptibility model of debris flows in Southwest China was proposed in this work. The following conclusions can be drawn:

1) According to the topography and geomorphology characteristics in Southwest China, the following nine indexes were used as evaluation factors of debris flow initiation susceptibility: the catchment area, longitudinal gradient, average gradient of the slope on both sides of the gully, catchment morphology, valley orientation, loose material reserves, location of the main loose material, antecedent precipitation, and rainfall intensity.

2) 70 typical debris flow gullies distributed along the Brahmaputra River, Nujiang River, Yalong River, Dadu River, and Ming River were investigated as statistical samples. The parameters of the prediction model were obtained based on the Hayashi's quantitative theory and regression analysis.

3) The proposed model was applied to analyze the initiation susceptibility of 10 debris flow gullies located on the upstream of the Dadu River, and the result showed that the judgment coincidence rate is 90%, indicating that the proposed model can accurately predict the initiation susceptibility of debris flow gullies in Southwest China.

Author contribution

FJ developed the model, RL did the field investigation, ZD prepared the manuscript with contributions from all co-authors.

Competing interests

The authors declare that they have no conflict of interest.

Acknowledgments:

The presented work was supported by the Sichuan Science and Technology Program (2018JY0471), and Sichuan Provincial Youth Science and Technology Innovation Team Special Projects of China (No. 2017TD0018), the Open Fund of Key Laboratory of Geological Hazards on Three Gorges Reservoir Area (China Three Gorges University) (2018KDZ01), Ministry of Education, and the JSPS Grant-in-Aid for Early Career Scientists (19K14804).

References

Beguería, S., Van Asch, T. W., Malet, J. P., and Gröndahl, S.: A GIS-based numerical model for simulating the kinematics of mud and debris flows over complex terrain, Nat. Hazards Earth Syst. Sci., 9, 1897–1909, https://doi.org/10.5194/nhess-9-1897-2009, 2009.

Bertrand, M., Liébault, F., and Piégay, H.: Debris-flow susceptibility of upland catchments, Nat. Hazards, 67(2), 497–511, https://doi.org/10.1007/s11069-013-0575-4, 2013.

Blahut, J., van Westen, C. J., and Sterlacchini, S.: Analysis of landslide inventories for accurate prediction of debris-flow source areas, Geomorphology, 119(1–2), 36–51, https://doi.org/10.1016/j.geomorph.2010.02.017, 2010.

Cama, M.; Lombardo, L., Conoscenti, C., and Rotigliano, E.: Improving transferability strategies for debris flow susceptibility assessment: Application to the Saponara and Itala catchments (Messina, Italy), Geomorphology, 288, 52–65, https://doi.org/10.1016/j.geomorph.2017.03.025, 2017.

Carrara, A., Crosta, G., and Frattini, P.: Comparing models of debris-flow susceptibility in the alpine environment, Geomorphology, 94(3–4), 353–378, https://doi.org/10.1016/j.geomorph.2006.10.033, 2008.

Dai, Z., Huang, Y., Cheng, H., and Xu, Q.: SPH model for fluid–structure interaction and its application to debris flow impact estimation, Landslides, 14(3), 917–928, https://doi.org/10.1007/s10346-016-0777-4, 2017.

Di, B. F., Zhang, H. Y., Liu, Y. Y., Li, J. R., Chen, N. S., Stamatopoulos, C.A., Luo, Y.Z., Zhan, Y.: Assessing Susceptibility of Debris Flow in Southwest China Using Gradient Boosting Machine, Sediment Res., 9: 12532, https://doi.org/10.1038/s41598-019-48986-5, 2019.

Gregoretti, C., Degetto, M., and Boreggio, M.: GIS-based cell model for simulating debris flow runout on a fan, J. Hydrol., 534, 326–340, https://doi.org/10.1016/j.jhydrol.2015.12.054, 2016.

Hayashi, C.: Sample survey and theory of quantification, Bull. Inter. Stat. Inst., 38, 505–514, 1961.

Horton, P., Jaboyedoff, M., Rudaz, B. E. A., and Zimmermann, M.: Flow-R, a model for susceptibility mapping of debris flows and other gravitational hazards at a regional scale, Nat. Hazards Earth Syst. Sci., 13(4), 869–885, https://doi.org/10.5194/nhess-13-869-2013, 2013.

Huang, Y., Cheng, H., Dai, Z., Xu, Q., Liu, F., Sawada, K., Moriguchi, S., and Yashima, A. SPH-based numerical simulation of catastrophic debris flows after the 2008 Wenchuan earthquake, B. Eng. Geol. Environ., 74(4), 1137–1151, https://doi.org/10.1007/s10064-014-0705-6, 2015.

Hürlimann, M., Abancó, C., and Moya, J.: Rockfalls detached from a lateral moraine during spring season. 2010 and 2011 events observed at the Rebaixader debris-flow monitoring site (Central Pyrenees, Spain), Landslides, 9(3), 385–393, https://doi.org/10.1007/s10346-011-0314-4, 2012.

Inoue H., Tabata H., and Tsuji H.: Emotion color combination models using the quantification theory type I and its application to uniform color combination, Transactions of Japan Society of Kansei Engineering, 8(3): 775–781, 2009. (in Japanese)

Ishihara, S., Nagamachi, M., and Ishihara, K.: Analyzing Kansei and design elements relations with PLS. In 10th Quality Management and Organiqatinal Development (QMOD) Conference, Helsingborg, Sweden, 18–20 June 2007, No.026, 2007.

Jomelli, V., Pavlova, I., Eckert, N., Grancher, D., and Brunstein, D.: A new hierarchical Bayesian approach to analyse environmental and climatic influences on debris flow occurrence, Geomorphology, 250, 407–421, https://doi.org/10.1016/j.geomorph.2015.05.022, 2015.

Kang, S., and Lee, S. R.: Debris flow susceptibility assessment based on an empirical approach in the central region of South Korea, Geomorphology, 308, 1–12, https://doi.org/10.1016/j.geomorph.2018.01.025, 2018.

Kappes, M. S., Malet, J. P., Remaître, A., Horton, P., Jaboyedoff, M., and Bell, R.: Assessment of debris-flow susceptibility at medium-scale in the Barcelonnette Basin, France. Nat. Hazards Earth Syst. Sci., 11(2), 627–641, https://doi.org/10.5194/nhess-11-627-2011, 2011.

Li, Y., Wang, H., Chen, J., and Shang, Y.: Debris flow susceptibility assessment in the Wudongde Dam area, China based on rock engineering system and fuzzy C-means algorithm, Water, 9(9), 669, https://doi.org/10.3390/w9090669, 2017.

Liu, G., Dai, E., Xu, X., Wu, W., and Xiang, A.: Quantitative assessment of regional debris-flow risk: a case study in Southwest China. Sustainability, 10(7), 2223, https://doi.org/10.3390/su10072223, 2018.

Lucà, F., Conforti, M., and Robustelli, G.: Comparison of GIS-based gullying susceptibility mapping using bivariate and multivariate statistics: Northern Calabria, South Italy, Geomorphology, 134(3–4), 297–308, https://doi.org/10.1016/j.geomorph.2011.07.006, 2011.

Matsumura, T.: Analysis of ovipositional environment using Quantification Theory Type I: the case of the butterfly, Luehdorfia puziloi inexpecta (Papilionidae). J. Insect Conserv., 8(1), 59–67, https://doi.org/10.1023/B:JICO.0000027509.99459.b5, 2004.

Moraci, N., Mandaglio, M. C., Gioffrè, D., and Pitasi, A.: Debris flow susceptibility zoning: an approach applied to a study area, Riv. Ital. Geotec., 51(2), 47–62, https://doi.org/10.19199/2017.2.0557-1405.047, 2017.

Prieto, J. A., Journeay, M., Acevedo, A. B., Arbelaez, J. D., and Ulmi, M.: Development of structural debris flow fragility curves (debris flow buildings resistance) using momentum flux rate as a hazard parameter, Eng. Geol., 239, 144–157, https://doi.org/10.1016/j.enggeo.2018.03.014, 2018.

Pirulli, M., and Sorbino, G.: Assessing potential debris flow runout: a comparison of two simulation models, Nat. Hazards Earth Syst. Sci., 8, 961–971, https://doi.org/10.5194/nhess-8-961-2008, 2008.

Rosatti, G., Zorzi, N., Zugliani, D., Piffer, S., and Rizzi, A.: A Web Service ecosystem for high-quality, cost-effective debris-flow hazard assessment. Environ. Model. Softw., 100, 33–47, https://doi.org/10.1016/j.envsoft.2017.11.017, 2018.

Schürch, P., Densmore, A. L., Rosser, N. J., and McArdell, B. W.: Dynamic controls on erosion and deposition on debris-flow fans, Geology, 39(9), 827–830, https://doi.org/10.1130/G32103.1, 2011.

Shen K. S., and Chen, K. H.: Exploring the Critical Appeal of Mobility-Augmented Reality Games, International Conference on Kansei Engineering & Emotion Research, Kuching, Sarawak, Malaysia, 19-22 March 2018, 451–459, 2018.

Shieh, C. L., Chen, Y. S., Tsai, Y. J., and Wu, J. H.: Variability in rainfall threshold for debris flow after the Chi-Chi earthquake in central Taiwan, China, Int. J. Sediment Res., 24(2), 177–188, https://doi.org/10.1016/S1001-6279(09)60025-1, 2009.

Suzen, L. M., and Doyuran, V.: A comparison of the GIS based landslide susceptibility assessment methods: multivariate versus bivariate, Environ. Geol., 45, 665–679, https://doi.org/10.1007/s00254-003-0917-8, 2004.

Brayshaw, D., and Hassan, M. A.: Debris flow initiation and sediment recharge in gullies, Geomorphology, 109(3–4), 122–131, https://doi.org/10.1016/j.geomorph.2009.02.021, 2009.

Wang, Q., Kong, Y., Zhang, W., Chen, J., Xu, P., Li, H., Xue, y., Yuan, X., Zhan J., and Zhu, Y.: Regional debris flow susceptibility analysis based on principal component analysis and self-organizing map: a case study in Southwest China, Arab. J. Geosci., 9(18), 718, https://doi.org/10.1007/s12517-016-2752-8, 2016.

Wu, S., Chen, J., Xu, C., Zhou, W., Yao, L., Yue, W., and Cui, Z.: Susceptibility Assessments and Validations of Debris-Flow Events in Meizoseismal Areas: Case Study in China's Longxi River Watershed, Nat. Hazards Rev., 21(1), 05019005, https://doi.org/10.1061/(ASCE)NH.1527-6996.0000347, 2020.

Wu, S., Chen, J., Zhou, W., Iqbal, J., and Yao, L.: A modified Logit model for assessment and validation of debris-flow susceptibility, B. Eng. Geol. Environ., 78(6), 4421–4438, https://doi.org/10.1007/s10064-018-1412-5, 2019.

Xu, Q., Zhang, S., Li, W. L., and Van Asch, T. W.: The 13 August 2010 catastrophic debris flows after the 2008 Wenchuan earthquake, China, Nat. Hazards Earth Syst. Sci., 12, 201–216, https://doi.org/10.5194/nhess-12-201-2012, 2012.

Xu, W., Yu, W., Jing, S., Zhang, G., and Huang, J.: Debris flow susceptibility assessment by GIS and information value model in a large-scale region, Sichuan Province (China), Nat. Hazards, 65(3), 1379–1392, 10.1007/s11069-012-0414-z, 2013.

Zou, Q., Cui, P., He, J., Lei, Y., and Li, S.: Regional risk assessment of debris flows in China-An HRU-based approach, Geomorphology, 340, 84–102, 10.1016/j.geomorph.2019.04.027, 2019.

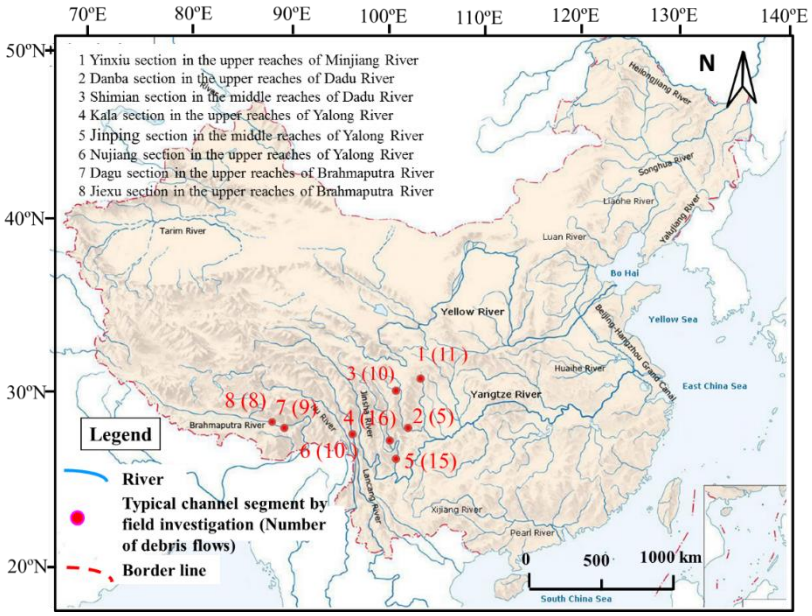

Figure 1: Distribution of the 70 debris flow gullies investigated in Southwest China (the base map is from Zhao 2014).

Figure 2: Typical debris flows in the study area. a) Morphology of the Xianwei Gully along the Yalong River; b) Moraine at the source of the Jiuzhui gully along the Brahmaputra; c) Loose material in the Jiaer gully along the Yalong River; d) Gravelly soil mixed with boulder in Sezu gully along the Dadu River.

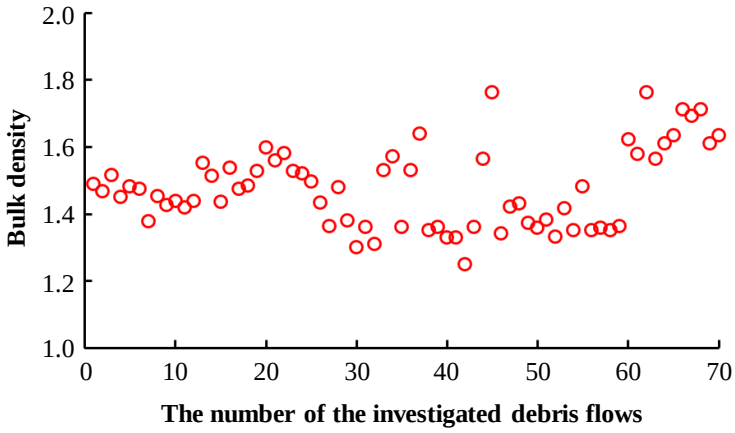

Figure 3: Density characteristics of the debris flow deposit in the study area.

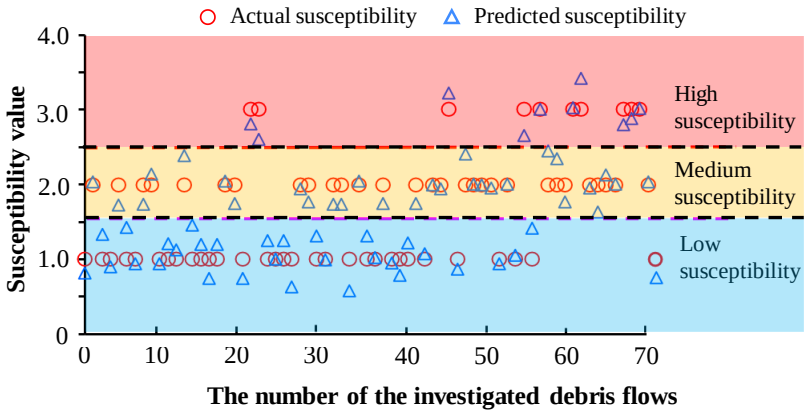

Figure 4: Comparison of actual susceptibility and predicted actual susceptibility.

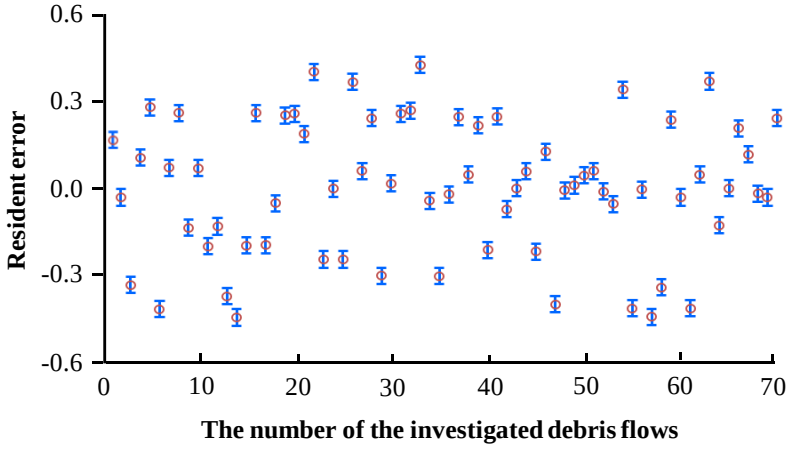

Figure 5: Residual distribution in the regression model of debris flow susceptibility.

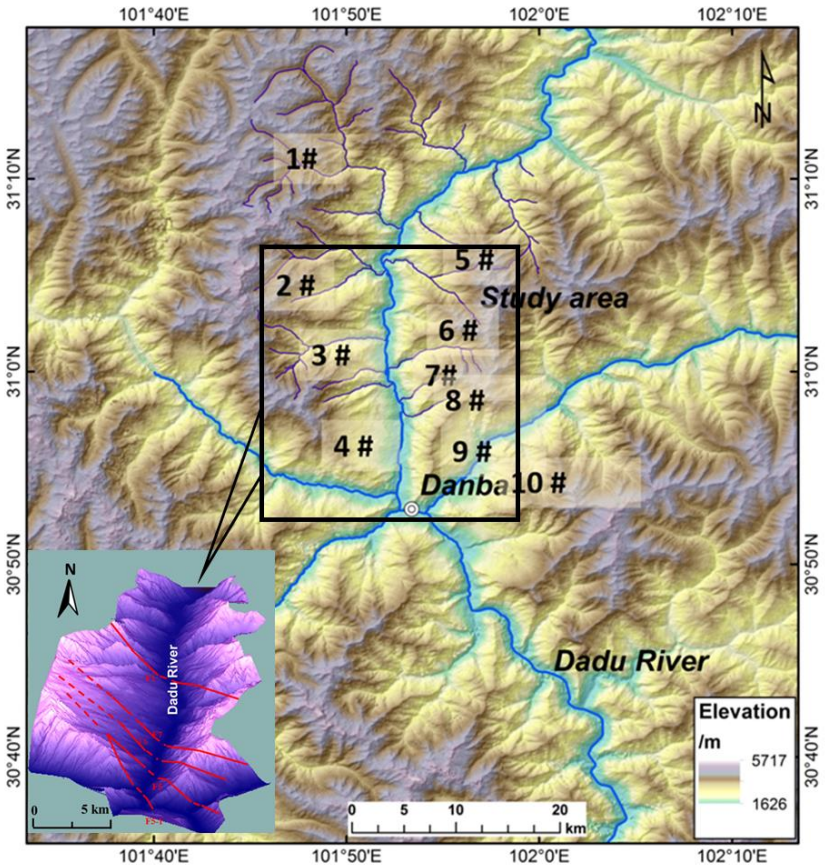

Figure 6: Distribution of debris flow gullies in Dadu river basin.

Figure 7: Typical characteristics of Danba section in upper reaches of Dadu River. a) Geomorphology of Bawang Gully; b) Loose deposits in the Mueryue Gully; c) Loose deposits on the trench bed of Shuikazi Gully; d) Abundant source material in the Qiongshan Gully.

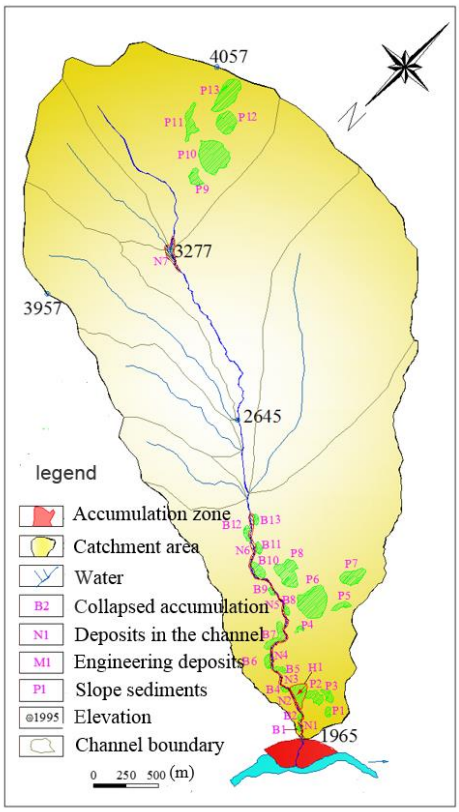

Figure 8: Distribution of loose deposits of Linong gully

Figure 9: Soil material in the Linong Gully deposit

Table 1 Qualitative grading criteria of antecedent precipitation

Classification	Standard of classification
Inadequacy	There is no antecedent precipitation or very little antecedent precipitation, which is not enough to make the surface soil moist.
Medium	The antecedent precipitation is intermittent or less, the soil is wet or muddy.
Adequacy	The precipitation lasts for several days, and the soil layer is full of water. Water accumulated in some low-lying areas, and the drainage is not smooth.

Table 2 Information and results of the geological drilling in the study area

No.	River	Debirs flow gully	Coordinates	Drilling depth (m)	Soil characteristics exposed by drilling
1	Yalong River	Reshui Gully	101°16′42″E 28°24′08″N	15	The lithology is mainly metamorphic sandstone and carbonaceous slate, with a small amount of quartzite. The percentage of boulder and gravel is about 40%, which is slightly angular. Their particle sizes are 40-60cm and 4-9cm, respectively. The rest material is silty clay with medium dense. The cementation state of the soil material in this area is good.
2	Yalong River	Reshui Gully	101°16′44″E 28°24′10″N	22	
3	Yalong River	Reshui Gully	101°16′45″E 28°24′12″N	26	
4	Yalong River	Shangtian Gully	101°16′26″E 28°24′08″N	21	The lithology is gravel soil with medium dense. The percentage of gravel and coarse sand are 43% and 20%, and the rest of the material is clay. The average thickness of the deposit in this area is about 19.0m.
5	Yalong River	Shangtian Gully	101°16′29″E 28°24′11″N	17	
6	Dadu River	Shuikazi Gully	101°52′07″E 31°03′38″N	31	The thickness of upper layer of the deposit is about 1.5 m, and the material is weak cemented silty clay with a small amount of gravel. The thickness of middle layer is about 2.0 m, the material is clay mixed with gravel, containing a small amount of boulder. The particle size of the gravel, breccia, and boulder are 2-3 cm, 10 cm, and 40 cm, respectively. The soil content in this layer is up to 70%. The lower layer is mainly composed of gravel and sand, and the particle size is relatively uniform, generally 5-8 cm. The roundness of the particles is good, and the content of fine particles is low.
7	Dadu River	Shuikazi Gully	101°52′09″E 31°03′39″N	36	
8	Dadu River	Shuikazi Gully	101°52′11″E 31°03′41″N	35	
9	Dadu River	Kaka Gully	101°52′12″E 31°00′11″N	21	The lithology is mainly mica quartz schist, which is slightly angular, grayish yellow, dry, and medium dense. The particle size of the boulder is 20-40 cm, accounting for about 40%. The boulder layer in this gully is mainly filled with silt and a small amount of gravel.
10	Dadu River	Kaka Gully	101°52′14″E 31°00′15″N	19	
11	Brahmaputra River	Menda Gully	92°25′12″E 29°15′22″N	22	The deposit in this area is mainly composed of gravelly soil mixed with boulder. The average

12	Brahmaputra River	Menda Gully	92°25′11″E 29°15′23″N	26	particle size of the gravels is 15-20 cm, accounting for about 40%. The average particle size of block stone is about 40-60 cm, accounting for about 10%-20%. In addition, there are some sporadic boulders with the average particle size of 3-4m.
13	Brahmaputra River	Menda Gully	92°25′13″E 29°15′24″N	29	
14	Brahmaputra River	Zhuangnan Gully	92°24′23″E 29°15′39″N	16	The material is mainly composed of dense gravelly soil and a small amount of silt. The gravels with the average particle size of 30-60 cm account for about 30%. The gravels with the average particle size of 15 cm account for about 10%. The rest is breccia soil, which has poor sorting performance and obvious miscellaneous accumulation characteristics.
15	Brahmaputra River	Zhuangnan Gully	92°24′24″E 29°15′41″N	11	
16	Brahmaputra River	Zhuangnan Gully	92°24′21″E 29°15′42″N	17	
17	Minjiang River	Banzi Gully	103°31'49"E 31°24'25"N	18	The deposit in this area is mainly composed of brown yellow gravel soil, which contains 10% cobble, 45% gravels, and 20% coarse sand, and the rest is clay.
18	Minjiang Rive	Banzi Gully	103°31'51"E 31°24'27"N	24	
19	Minjiang Rive	Chutou Gully	103°29'12"E 31°20'21"N	14	The deposit zone in this area is 150 m long and 100 m wide. The soil material is medium dense, which contains 30% boulder and 70% gravelly soil.
20	Minjiang Rive	Chutou Gully	103°29'13"E 31°20'22"N	17	
21	Minjiang Rive	Chutou Gully	103°29'14"E 31°20'25"N	13	

Table 3 Nine indexes used in the prediction model of debris flow susceptibility

Symbol	Physical significance
x_1	Catchment area (km^2)
x_2	Longitudinal gradient (‰)
x_3	Average gradient of slope on both sides of gully (°)
x_4	Catchment morphology
x_5	Valley orientation
x_6	Loose Material reserves ($10^4\ m^3/km^2$)
x_7	Main loose material position
x_8	Antecedent precipitation
x_9	H_{1p} rainfall intensity (mm)

Table 4 Grading criteria of the evaluation indexes in the prediction model of debris flow susceptibility

Item	Category	Value	Item	Category	Value
Catchment area x_1 (km^2)	x_{11}	< 1 km^2	Valley orientation x_5 (/)	x_{51}	Sunny slope
	x_{12}	1–10 km^2		x_{52}	Shady slope
	x_{13}	10–100 km^2	Loose material reserves x_6 (10^4 m^3/km^2)	x_{61}	< 1×10^4 m^3/km^2
	x_{14}	≥100 km^2		x_{62}	1–5×10^4 m^3/km^2
Longitudinal gradient x_2 (‰)	x_{21}	< 100‰		x_{63}	≥ 5×10^4 m^3/km^2
	x_{22}	100‰–300‰	Main loose material position x_7 (/)	x_{71}	Upstream or tributary
	x_{23}	≥300‰		x_{72}	Middle and lower reaches
Average gradient of slope on both sides of gully x_3 (°)	x_{31}	< 30		x_{73}	Toe of gully
	x_{32}	30–40°	Antecedent precipitation x_8 (/)	x_{81}	Inadequacy
	x_{33}	≥40°		x_{82}	Medium
Catchment morphology x_4 (/)	x_{41}	Z < 0.3		x_{83}	Adequacy
	x_{42}	Z = 0.3–0.7	H_{1p} rainfall intensity x_9 (mm)	x_{91}	< 30 mm
	x_{43}	$Z \geq 0.7$		x_{92}	≥ 30 mm

Note: Z is the length to width ratio of the debris gully

Table 5 Sample data for debris flow examples from Southwest China

No.	x_1	x_2	x_3	x_4	x_5	x_6	x_7	x_8	x_9	Susceptibility
1	0.77	567	35	Long strip	SE	8.05	Upstream	Inadequacy	26.38	Low
2	13.3	366	28	Ellipse	SE	10.04	Upstream	Inadequacy	26.38	Medium
3	2.62	624	37	Long strip	SE	4.39	Upstream	Inadequacy	26.38	Low
4	2.47	624	36	Long strip	SE	26.06	Middle and lower reaches	Inadequacy	26.38	Low
5	71.64	194	22	Ellipse	S	8.06	Upstream	Inadequacy	26.38	Medium
6	18.89	344	35	Suborbicular	NE	3.08	Upstream	Inadequacy	26.38	Low
7	13.01	404	36	Ellipse	NW	3.43	Upstream	Inadequacy	26.38	Low
8	43.51	199	28	Suborbicular	NE	4.01	Upstream	Inadequacy	26.38	Medium
9	38.4	251	37	Long strip	SE	5.38	Upstream	Inadequacy	26.38	Medium
10	4.04	412.53	37	Long strip	NE	6.15	Upstream	Inadequacy	26.38	Low
11	1.39	480	35	Long strip	N	7.85	Upstream	Inadequacy	26.38	Low
12	1.62	569.4	36	Long strip	S	19.11	Middle and lower reaches	Inadequacy	26.38	Low
13	13.23	280.61	31	Ellipse	N	3.07	Middle and lower reaches	Inadequacy	26.38	Medium
14	2.48	536.68	41	Long strip	S	22.63	Upstream	Inadequacy	26.38	Low
15	5.15	507.69	39	Ellipse	S	10.74	Upstream	Inadequacy	26.38	Low
16	1.25	630.34	43	Suborbicular	NE	6.44	Middle and lower reaches	Inadequacy	26.38	Low
17	135.6	139.46	30	Suborbicular	NE	3.91	Upstream	Inadequacy	26.38	Low
18	53.42	169.87	30	Ellipse	SW	1.89	Middle and lower reaches	Adequacy	32.85	Medium
19	169.72	121.62	25	Ellipse	S	0.98	Branch trench、Upstream	Adequacy	32.85	Medium
20	15.53	171.2	36	Long strip	N	3.24	Upstream	Adequacy	32.85	Low
21	31.35	171	33	Ellipse	NE	2.74	Middle and lower reaches	Adequacy	32.85	High
22	7.37	462.11	35	Suborbicular	NE	7.06	Middle and lower reaches	Adequacy	32.85	High
23	20.99	235.79	25	Ellipse	SW	1.47	Upstream	Adequacy	32.85	Low
24	275.41	60	23	Ellipse	SE	0.89	Upstream	Adequacy	32.85	Low

No.	x_1	x_2	x_3	x_4	x_5	x_6	x_7	x_8	x_9	Susceptibility
25	211.4	94	34	Ellipse	NW	1.04	Tributary	Medium	32.85	Low
26	8.89	256	36	Long strip	SW	3.79	Upstream	Adequacy	32.85	Low
27	28.91	190	31	Ellipse	SE	2.20	Middle and lower reaches	Adequacy	32.85	Medium
28	34.84	158	43	Long strip	SW	0.90	Middle and lower reaches	Adequacy	42.2	Medium
29	102.7	110	29	Long strip	NE	0.75	Middle and lower reaches	Adequacy	42.2	Low
30	84.81	146.2	32	Ellipse	NE	0.78	Branch trench	Adequacy	42.2	Low
31	132.02	129.5	35	Ellipse	SW	0.42	Upstream	Adequacy	42.2	Medium
32	5.5	318.01	33	Ellipse	NE	6.37	Middle and lower reaches	Adequacy	42.2	Medium
33	124.3	117.9	26	Ellipse	SW	1.37	Branch trench, Upstream	Adequacy	42.2	Low
34	26.2	203.9	36	Ellipse	SE	3.85	Upstream	Adequacy	42.2	Medium
35	29.56	205.1	32	Long strip	SW	1.84	Upstream	Adequacy	42.2	Low
36	80.34	119.1	38	Long strip	NE	1.51	Branch trench, Upstream	Adequacy	42.2	Low
37	8.45	301.5	37	Ellipse	NE	2.06	Upstream	Adequacy	42.2	Medium
38	16.26	217.1	36	Long strip	SE	1.15	Branch trench, Upstream	Adequacy	42.2	Low
39	77.5	138.5	41	Long strip	NE	1.22	Upstream	Adequacy	42.2	Low
40	23.1	235.52	24	Long strip	SW	1.68	Upstream	Adequacy	42.2	Low
41	47.01	166	30	Ellipse	NE	1.69	Toe of gully	Adequacy	42.2	Medium
42	83.11	125	31	Ellipse	NE	0.40	Upstream	Adequacy	42.2	Low
43	21.11	238	32	Ellipse	SW	0.87	Upstream	Adequacy	42.2	Medium
44	73.11	156	32	Ellipse	SE	1.10	Middle and lower reaches	Medium	43.12	Medium
45	64.7	144	33	Ellipse	NW	0.78	Toe of gully	Medium	43.12	High
46	21.87	242.95	36	Ellipse	NW	1.55	Branch trench, Upstream	Medium	43.12	Low
47	3.5	530.4	42	Ellipse	NW	8.34	Middle and lower reaches	Medium	43.12	Medium
48	26.66	296.6	33	Ellipse	SE	4.70	Middle and lower reaches	Medium	43.12	Medium
49	32.23	178.35	30	Suborbicular	S	5.91	Middle and lower reaches	Medium	28.47	Medium

No.	x_1	x_2	x_3	x_4	x_5	x_6	x_7	x_8	x_9	Susceptibility
50	40.03	164.6	31	Ellipse	SE	5.59	Middle and lower reaches	Medium	28.47	Medium
51	3.25	235.43	35	Ellipse	NW	2.18	Upstream	Medium	28.47	Low
52	351.2	92.4	24	Ellipse	S	10.37	Branch trench	Medium	28.47	Medium
53	8.85	220.35	36	Suborbicular	NW	4.01	Branch trench, Upstream	Medium	28.47	Low
54	25.31	203.62	30	Long strip	S	4.75	Middle and lower reaches	Medium	28.47	High
55	1.78	214.58	28	Suborbicular	NE	0.73	Upstream	Medium	28.47	Low
56	5.8	246.48	34	Ellipse	SW	15.79	Middle and lower reaches	Medium	28.47	High
57	7.6	230.09	42	Ellipse	S	17.34	Middle and lower reaches	Medium	28.47	Medium
58	1.7	140.37	36	Long strip	SE	136.82	Middle and lower reaches	Medium	28.47	Medium
59	53.27	132.43	32	Ellipse	SE	10.33	Upstream	Medium	28.47	Medium
60	14.15	178.6	28	Suborbicular	SW	55.50	Middle and lower reaches	Adequacy	41.1	High
61	1.48	244.2	33	Suborbicular	SW	32.81	Middle and lower reaches	Adequacy	41.1	High
62	0.89	256.8	38	Suborbicular	SW	18.81	Middle and lower reaches	Adequacy	41.1	Medium
63	0.98	243.2	35	Suborbicular	SW	12.70	Middle and lower reaches	Adequacy	41.1	Medium
64	3.73	120	24	Long strip	SW	9.51	Upstream	Adequacy	41.1	Medium
65	3.37	450.9	40	Ellipse	SE	8.80	Upstream	Adequacy	41.1	Medium
66	0.57	207.7	31	Suborbicular	SW	36.89	Middle and lower reaches	Adequacy	41.1	High
67	3.02	488.8	42	Ellipse	SE	20.99	Middle and lower reaches	Adequacy	41.1	High
68	7.59	352	28	Ellipse	NE	19.26	Middle and lower reaches	Adequacy	41.1	High
69	32.04	223	23	Ellipse	NW	13.67	Middle and lower reaches	Adequacy	41.1	High
70	3.27	235	35	Ellipse	NE	9.29	Upstream	Adequacy	41.1	Low

Table 6 Score values of each index after normalization

Item	Category	Value	Item	Category	Value
Catchment area x_1 （km^2）	x_{11}	0.573	Valley orientation x_5	x_{51}	-0.136
	x_{12}	0.821		x_{52}	-0.174
	x_{13}	0.910	Loose material reserves x_6 （10^4 m^3/km^2）	x_{61}	0
	x_{14}	0		x_{62}	0.246
Longitudinal gradient x_2（‰）	x_{21}	0.875		x_{63}	0.454
	x_{22}	0.955	Main loose material position x_7	x_{71}	-0.220
	x_{23}	0.320		x_{72}	-0.161
Average gradient of slope on both sides of gully x_3（°）	x_{31}	0		x_{73}	0
	x_{32}	-0.107	Antecedent precipitation x_8	x_{81}	0
	x_{33}	0		x_{82}	0.034
Catchment morphology x_4	x_{41}	-0.163		x_{83}	0.071
	x_{42}	0.135	H_{1p} rainfall intensity x_9 （mm）	x_{91}	-0.038
	x_{43}	0.213		x_{92}	0.043

Table 7 Quantitative model eigenvalue

Model	R^2	Standard deviation
1	0.749	0.289

Table 8 Prediction model accuracy

Category	Low	Medium	High
Accuracy (%)	78.5	92.3	82.0

15 Table 9 Sample data from Kaka area in the upstream of Dadu River

No.	Ditch name	x_1	x_2	x_3	x_4	x_5	x_6	x_7	x_8	x_9
1	Luotuo	227.1	102	25	0.745	SE	0.87	Middle and lower	Adequacy	43.8
2	Qiongshan	84.90	200	28	0.907	SE	10.67	Middle and lower	Adequacy	43.8
3	Shuikazi	49.78	209	31	0.534	SE	4.82	Middle and lower	Adequacy	43.8
4	Bawang	11.84	310	32	0.219	SW	2.36	Upstream	Medium	43.8
5	Shenluo	4.54	455	33	0.580	NW	42.46	Toe of gully	Medium	43.8
6	Mueryue	35.81	206	36	0.376	NW	10.08	Upstream	Adequacy	43.8
7	Sezu	4.23	613	42	0.812	NW	26.24	Middle and lower	Adequacy	43.8
8	Muerluo	11.93	358	34	0.546	NW	9.98	Upstream	Medium	43.8
9	Yaneryan	30.01	242	34	0.382	SW	5.64	Middle and lower	Medium	43.8
10	Linong	10.09	332	35	0.448	NW	24.30	Middle and lower	Medium	43.8

Table 10 Comparison of predicted values and actual measured values

Number	**1**	**2**	**3**	**4**	**5**	**6**	**7**	**8**	**9**	**10**
Calculated *Y* value	2.562	1.805	1.764	2.540	2.748	2.167	1.705	1.843	1.348	2.421
Predicted susceptibility	High	Medium	Medium	High	High	Medium	Medium	Medium	Low	Medium
Geological judgment of actual susceptibility	High	Medium	Medium	High	High	Medium	Medium	Medium	Low	High
Result	Right	Right	Right	Right	Right	Right	Right	Right	Right	**Wrong**